Applications of Bilinear Control Theory in Nonlinear Spectroscopy

Kunal Marwaha*
Supervised by Prof. Birgitta Whaley†

University of California, Berkeley

May 11, 2016

Here, I motivate control-theoretic system identification techniques for 3rd order spectroscopy. I begin by deriving a recursive perturbative von Neumann equation, and constructing an extended Liouville space to define a bilinear evolution equation. Since the bilinear terms are short spectral-interaction pulses, I build on control-theoretic work by Juang and others [10, 11] to construct a linear equation for the third-order polarization signal. Thus, the classic inversion problem of determining Hamiltonian parameters given polarization output data is soluble. I show how to efficiently solve these equations in the forward direction and inversion direction for a dimer system.

1 Introduction

Many molecular experiments involve a Hamiltonian interaction term of the system with some light source, as in constructing quantum bits [17] and in understanding photosynthesis [8]. Methods to determine these Hamiltonian parameters are essential to characterizing each complex molecular system. Typically nicknamed the "inversion problem", the process of accurately estimating Hamiltonian parameters and transition dipole moments can be deceptively difficult, with few successful multiparameter approaches [5] [17]. Some of these measurements are conducted via nonlinear spectroscopy measurements [7]. In such measurements, one can directly measure the higher-order perturbative terms.

The most common method to estimate light-matter interaction dynamics is with a third-order polarization experiment [12]. In this four-wave mixing process, three successive pulses of light (at time t_0, t_1, t_2) are shined on a molecular system, causing some excitations. A final light-pulse (at time t_3) relaxes the molecular system, producing a light-pulse of some amplitude, dependent on the quantum state at that time. Varying the delays between successive light pulses ($t_1 - t_0, t_2 - t_1, t_3 - t_2$) changes the final quantum state (and thereby the amplitude of the emission pulse).

Generally, a table of data is produced for each system, discretizing over each time variable. This information is presented by conducting a Fourier transform on the first and last pulse delays ($t_1 - t_0, t_3 - t_2$) and constructing a 2D plot of the real part of the signal (with the axes as w_1 and w_3) [12]. Now, the polarization is a function of the middle pulse delay ($t_2 - t_1$), generating a 2D frequency-space plot for each choice of $t_2 - t_1$. Each data point is measured separately; that is, choosing ($t_1 - t_0, t_2 - t_1, t_3 - t_2$) will produce a complex-valued polarization scalar. A precise frequency-space plot requires many of these measurements.

One can qualitatively interpret from peaks and patterns in the frequency plots. Instead, I derive a new approach that borrows terminology from control theory, a formal method to characterize systems from input-output measurements [10]. The goal is to derive and solve a simple set of equations that can be inverted efficiently and quantitatively. This novel approach quickly generates a large amount of polarization data by simulating the forward evolution of the quantum state. Parameter estimation amounts to inverting these equations. Although the problem is non-convex, the inversion can be done with a variety of optimization techniques, including gradient descent and Alternating Direction Method of Multipliers (ADMM) [3] [14]. In this work, I show that physical parameters can be computationally determined, instead of visually estimated, through standard nonlinear spectroscopy experiments.

*electronic address: marwahaha@berkeley.edu
†Department of Chemistry, Berkeley Center for Quantum Information and Computation, University of California, Berkeley, California 94720, USA

2 Mathematics

2.1 Recursive Perturbative Equation of Motion

The von Neumann equation [4] describes time evolution of a density matrix $\hat{\rho} = \sum_i p_i \left|\psi_i\right\rangle \left\langle\psi_i\right|$, where $\{\left|\psi_i\right\rangle\}$ spans the Hilbert space, as

$$\frac{\partial \hat{\rho}}{\partial t} = -\frac{i}{\hbar}[\hat{H}(t), \hat{\rho}(t)] \,. \tag{1}$$

Integrating, one finds

$$\hat{\rho}(t) = \hat{\rho}(0) + \frac{-i}{\hbar}\int_0^t dt_1 [\hat{H}(t_1), \hat{\rho}(t_1)] \,. \tag{2}$$

This can be solved by repeatedly inserting the above equation into itself, as

$$\hat{\rho}(t) = \hat{\rho}(0) + \frac{-i}{\hbar}\int_0^t dt_1 [\hat{H}(t_1), \hat{\rho}(0)] + \left(\frac{-i}{\hbar}\right)^2 \int_0^t dt_1 \int_0^{t_1} dt_2 [\hat{H}(t_1), [\hat{H}(t_2), \hat{\rho}(t_2)]] \,. \tag{3}$$

And so on:

$$\hat{\rho}(t) = \hat{\rho}(0) + \sum_{n=1}^{\infty} \left(\frac{-i}{\hbar}\right)^n \int_0^t dt_1 \int_0^{t_1} dt_2 ... \int_0^{t_{n-1}} dt_n [\hat{H}(t_1), [\hat{H}(t_2), ...[\hat{H}(t_n), \hat{\rho}(t_n)]...]] \,. \tag{4}$$

This series is traditionally written as

$$\hat{\rho}(t) = \sum_{n=0}^{\infty} \hat{\rho}_n(t) = \hat{\rho}(0) + \sum_{n=1}^{\infty} \hat{\rho}_n(t) \,, \tag{5}$$

where $\hat{\rho}_0(t) = \hat{\rho}(0)$ and $\hat{\rho}_n(t) = \int_0^t dt_1 ... \int_0^{t_{n-1}} dt_n [\hat{H}(t_1), ...[\hat{H}(t_n), \hat{\rho}(t_n)]...]$.

Since the commutator is linear in each argument, the expression $\rho_n(t)$ can be written recursively, as

$$\hat{\rho}_n(t) = \frac{-i}{\hbar}\int_0^t d\tau [\hat{H}(\tau), \hat{\rho}_{n-1}(\tau)] \,. \tag{6}$$

Differentiating both sides, I derive an recursive equation of motion for the n^{th} order perturbation:

$$\frac{\partial \hat{\rho}_n(t)}{\partial t} = \frac{-i}{\hbar}[\hat{H}(t), \hat{\rho}_{n-1}(t)] \,. \tag{7}$$

2.2 Third-Order Polarization in an Extended Liouville Space

2.2.1 Hilbert, Liouville, Extended Liouville Space

If there are n energy levels in a quantum system, the Hilbert space $\mathbb{H}_n$ is an $n-$dimensional vector space that can be used to describe the quantum state and its evolution. In general, a density operator (or density matrix) describes the quantum state, denoted by $\hat{\rho}$. This is a linear operator in the Hilbert space, i.e. $\hat{\rho} \in \mathcal{L}(\mathbb{H}_n)$. The Hamiltonian $\hat{H} \in \mathcal{L}(\mathbb{H}_n)$ is an operator that evolves the quantum state as in equation 1. Often, when the Hamiltonian contains a small interaction term, $\hat{\rho}$ can be perturbatively expanded as in equation 5. So, $\hat{\rho}_i \in \mathcal{L}(\mathbb{H}_n)$ for each perturbative term $i \geq 0$. Other Hilbert-space operators that appear later include $\hat{U}$ (the propagator) and $\hat{\mu}$ (the transition dipole matrix).

Any Hilbert space can be converted into Liouville space $\mathbb{L}_{n^2}$. This n^2-dimensional vector space "vectorizes" each Hilbert space operator by stacking each entry of the $n \times n$ matrix representation into one $n^2 \times 1$ vector. So, $\left|\hat{\rho}\right\rangle, \left|\hat{\rho}_i\right\rangle, \left|\hat{\mu}\right\rangle$ are all vectors in Liouville space. One can create operators in this space, termed "superoperators", that evolve Liouville vectors. This can be a useful tool to linearize certain expressions. As shown in [1], the expression $\hat{A}\hat{\rho}\hat{B}^{\dagger}$ in Hilbert space is $(\hat{A} \otimes \hat{B})\left|\hat{\rho}\right\rangle$ in Liouville space, where $\otimes$ denotes the tensor product. The

commutator $[\hat{A}, \hat{\rho}]$ in Hilbert space is denoted $\hat{\hat{A}}\,|\hat{\rho}\rangle$ in Liouville space, where $\hat{\hat{A}} = \hat{A} \otimes \mathbb{1}_n - \mathbb{1}_n \otimes \hat{A}$. (When $\hat{A}$ is the Hamiltonian $\hat{H}$, this is called the "Liouvillian".) Any trace operation $tr(\hat{A}\hat{\rho})$ in Hilbert space is $\langle \hat{A} | \hat{\rho} \rangle$ in Liouville space [1].

It is useful to define a larger vector space $\mathbb{S}_{4n^2}$ (let's call it "extended Liouville space") to encapsulate the evolution of multiple perturbative components of $\hat{\rho}$ at once. In particular, this $4n^2-$dimensional space is the concatenation of four Liouville spaces; that is, $\mathbb{S}_{4n^2} = \mathbb{L}_{n^2} \oplus \mathbb{L}_{n^2} \oplus \mathbb{L}_{n^2} \oplus \mathbb{L}_{n^2}$ where $\oplus$ is the direct sum. I will use the state vector $\tilde{\mathbf{x}} \in \mathbb{S}_{4n^2}$, defined as

$$\tilde{\mathbf{x}}(t) = \begin{pmatrix} |\hat{\rho}_0(t)\rangle \\ |\hat{\rho}_1(t)\rangle \\ |\hat{\rho}_2(t)\rangle \\ |\hat{\rho}_3(t)\rangle \end{pmatrix} . \tag{8}$$

Vectors in the extended Liouville space $\mathbb{S}_{4n^2}$ will be in bold-face, like $\tilde{\mathbf{x}}$. There are operators of the extended Liouville space (let's call them "extended superoperators"); often I write them using the letters $\tilde{A}, \tilde{N}, \tilde{Q}$.

2.2.2 Nonlinear Spectroscopy in Extended Liouville Space

In nonlinear spectroscopy, polarization is related to the perturbation of the density matrix as follows [12]:

$$P(t) = \sum_{n=0}^{\infty} P_n(t) \tag{9}$$

$$P_n(t) = \langle \hat{\mu} \hat{\rho}_n(t) \rangle = tr(\hat{\mu} \hat{\rho}_n(t)) \tag{10}$$

The goal is to find a space where there is a simple relationship between $P_3(t)$ and $\hat{\rho}_n(t)$.

Consider the state vector $\tilde{\mathbf{x}} \in \mathcal{S}_{4n^2}$ defined in equation 8. I encode the recursive perturbative evolution equations (equation 5) as an extended superoperator. Explicitly, $\tilde{\mathbf{x}}(t)$ is governed by

$$\frac{\partial \tilde{\mathbf{x}}(t)}{\partial t} = \begin{pmatrix} 0 & 0 & 0 & 0 \\ \hat{\hat{M}}(t) & 0 & 0 & 0 \\ 0 & \hat{\hat{M}}(t) & 0 & 0 \\ 0 & 0 & \hat{\hat{M}}(t) & 0 \end{pmatrix} \tilde{\mathbf{x}}(t) \,, \tag{11}$$

where $\tilde{\mathbf{x}} = \begin{pmatrix} |\hat{\rho}(0)\rangle & 0 & 0 & 0 \end{pmatrix}^\top$ and $\hat{\hat{M}}(t) \in \mathcal{L}(\mathbb{L}_{n^2})$ is equal to $\frac{-i}{\hbar}\hat{\hat{H}}(t)$, where $\hat{\hat{H}}(t)$ is the Liouvillian. Recall that the Liouvillian $\hat{\hat{H}}(t)\cdot$ corresponds to the commutator $[\hat{H}(t), \cdot]$ in Hilbert space.

Similarly, the third-order polarization $P_3(t)$ is the inner product of $\tilde{\mathbf{x}}$ with some vector $\tilde{\mathbf{C}} \in \mathbb{S}_{4n^2}$. Thus, $\tilde{\mathbf{C}}$ is

$$\tilde{\mathbf{C}} = \begin{pmatrix} 0 \\ 0 \\ 0 \\ |\hat{\mu}\rangle \end{pmatrix} , \tag{12}$$

where $|\hat{\mu}\rangle \in \mathbb{L}_{n^2}$ is the transition dipole matrix from the Hilbert space, "vectorized" into Liouville space. In short,

$$P_3(t) = \tilde{\mathbf{C}}^\dagger \tilde{\mathbf{x}} = \langle \hat{\mu} | \hat{\rho}_3(t) \rangle = tr(\hat{\mu} \hat{\rho}_3(t)) \,. \tag{13}$$

Equation 11 is a first-order linear differential equation describing the evolution of $\tilde{\mathbf{x}}$ (and thus $\hat{\rho}_n(t)$). Equation 13 is a measurement protocol to construct $P_3(t)$ from $\tilde{\mathbf{x}}$.

There is a natural progression from operators to superoperators to extended superoperators, where operator in Hilbert space vectorize in Liouville space (i.e. $\hat{\rho}$ becomes $|\hat{\rho}\rangle$, and four vectors in Liouville space concatenate into one vector in extended Liouville space. I henceforth drop extraneous symbols from vectors and matrices. Vectors in extended Liouville space will remain in bold-face.

2.3 The Interaction Frame

2.3.1 Converting to the Interaction Frame

In nonlinear spectroscopy, our Hamiltonian looks like the following:

$$H(t) = H_0 + \vec{E}(t) \cdot \vec{\mu} \tag{14}$$

$$= H_D + H_\delta + \vec{E}(t) \cdot \vec{\mu} \tag{15}$$

Here, H_0 is the electric-field independent component, consisting of H_D (a diagonal matrix) and H_δ (a general matrix). I shift into the interaction frame (also referred to as interaction picture or Dirac picture) to simplify:

$$U = e^{\frac{i}{\hbar} H_D t} \tag{16}$$

$$\rho^I(t) = U\rho(t)U^\dagger = U\left(\sum_{i=0}^{\infty} \rho^i(t)\right) U^\dagger \tag{17}$$

$$\rho_n^I(t) = U\rho_n(t)U^\dagger \qquad (\forall n \geq 0) \tag{18}$$

Note that U is unitary, so its inverse U^{-1} is its conjugate transpose $U^\dagger$. This operator is responsible for converting vectors and operators in Hilbert space into the interaction frame. The inverse process is straightforward:

$$\rho(t) = U^\dagger \rho^I(t) U \,. \tag{19}$$

As mentioned in section 2.2, any expression $U\rho U^\dagger$ in Hilbert space is $(U \otimes U)\,|\rho\rangle$ in Liouville space [1]. The superoperator $(U \otimes U)$ converts the density matrix to the interaction frame in Liouville space.

$$|\rho^I(t)\rangle = (U \otimes U)\,|\rho(t)\rangle \tag{20}$$

$$|\rho_n^I(t)\rangle = (U \otimes U)\,|\rho_n(t)\rangle \qquad (\forall n \geq 0) \tag{21}$$

The state vector $\mathbf{x}$ from extended Liouville space transforms the same way as $\rho(t)$. I define the extended superoperator $Q_D(t)$ as

$$Q_D(t) = \mathbb{1}_4 \otimes (U \otimes U) = \begin{pmatrix} U \otimes U & 0 & 0 & 0 \\ 0 & U \otimes U & 0 & 0 \\ 0 & 0 & U \otimes U & 0 \\ 0 & 0 & 0 & U \otimes U \end{pmatrix} . \tag{22}$$

Note that $Q_D(t)$ converts $\mathbf{x}$ into the interaction frame:

$$\mathbf{x}^I(t) = Q_D(t)\mathbf{x}(t) \,. \tag{23}$$

Since $U \otimes U$ and $Q_D(t)$ are also unitary, it's easy to convert out of the interaction frame:

$$|\rho(t)\rangle = (U \otimes U)^\dagger\,|\rho^I(t)\rangle = (U^\dagger \otimes U^\dagger)\,|\rho^I(t)\rangle \tag{24}$$

$$\mathbf{x}(t) = Q_D^\dagger(t)\mathbf{x}^I(t) \tag{25}$$

Each of U, $U \otimes U$, and $Q_D(t)$ are all diagonal, since they are constructed from a diagonal H_D.

2.3.2 Evolution in the Interaction Frame

The density operator evolves slightly differently in this frame, since $\frac{\partial}{\partial t}\rho^I(t) = \dot{U}\rho(t)U^\dagger + U\dot{\rho}(t)U^\dagger + U\rho(t)\dot{U^\dagger}$. The first and last terms are easy to solve, since $U^{-1} = U^\dagger$ is unitary:

$$i\hbar\frac{\partial}{\partial t}U = i\hbar\dot{U} = i\hbar\frac{i}{\hbar}H_D U = -UH_D \tag{26}$$

$$i\hbar\left(\dot{U}\rho(t)U^\dagger + U\rho(t)\dot{U^\dagger}\right) = UH_D\rho(t)U^\dagger - U\rho(t)H_D U^\dagger = -UH_D U^\dagger U\rho(t)U^\dagger + U\rho(t)U^\dagger H_D U^\dagger \tag{27}$$

$$= -[UH_D U^\dagger, U\rho(t)U^\dagger] = -[UH_D U^\dagger, \rho^I(t)] \tag{28}$$

The middle term is also simple, by the von Neumann equation (equation 1):

$$i\hbar\left(U\frac{\partial\rho(t)}{\partial t}U^\dagger\right) = i\hbar\left(U\dot{\rho(t)}U^\dagger\right) = i\hbar\left(\frac{-i}{\hbar}U[H(t),\rho(t)]U^\dagger\right) = U\left(H(t)\rho(t)-\rho(t)H(t)\right)U^\dagger \tag{29}$$

$$= UH(t)U^\dagger U\rho(t)U^\dagger - U\rho(t)U^\dagger UH(t)U^\dagger = [UH(t)U^\dagger, U\rho(t)U^\dagger] = [UH(t)U^\dagger, \rho^I(t)] \tag{30}$$

Thus, putting the terms together, I derive the interaction-frame evolution equation:

$$i\hbar\frac{\partial\rho^I(t)}{\partial t} = -[UH_DU^\dagger,\rho^I(t)] + [UH(t)U^\dagger,\rho^I(t)] = [U\left(H_\delta + \vec{E}(t)\cdot\vec{\mu}\right)U^\dagger,\rho^I(t)] \tag{31}$$

$$\frac{\partial\rho^I(t)}{\partial t} = -\frac{i}{\hbar}[H^I(t),\rho^I(t)] \tag{32}$$

Here, I have implicitly defined the interaction Hamiltonian $H^I(t) = U\left(H_\delta + \vec{E}(t)\cdot\vec{\mu}\right)U^\dagger$. Using the results from section 2.1, I conclude

$$\frac{\partial\rho^I_n(t)}{\partial t} = -\frac{i}{\hbar}[H^I(t),\rho^I_{n-1}(t)]\,. \tag{33}$$

I will now investigate the effect of the rotating wave approximation on a dimer system.

2.4 The Rotating Wave Approximation for a Dimer System

The rotating wave approximation neglects quickly-oscillating terms when a perturbation is small compared to the free evolution of a quantum [16]. This can simplify expressions and will make our derivation easier. It consists of switching into the interaction frame (also known as the rotating frame or Dirac picture) and neglecting any counter-resonant terms.

A dimer system has two sites that can be excited, with energy levels E_a and E_b. I look at a four-dimensional Hilbert space in this site basis. The associated basis vectors are $[|gg\rangle, |eg\rangle, |ge\rangle, |ee\rangle]$, where $|g\rangle$ is the ground state and $|e\rangle$ is the excited state. Then,

$$H_0 = H_D + H_\delta \tag{34}$$

$$= \begin{pmatrix} 0 & 0 & 0 & 0 \\ 0 & E_0 & 0 & 0 \\ 0 & 0 & E_0 & 0 \\ 0 & 0 & 0 & 2E_0 \end{pmatrix} + \begin{pmatrix} 0 & 0 & 0 & 0 \\ 0 & \Delta E & J & 0 \\ 0 & J & -\Delta E & 0 \\ 0 & 0 & 0 & 0 \end{pmatrix}, \tag{35}$$

where $E_0 = \hbar w_0 = \frac{E_a+E_b}{2}$ is the average energy, $\Delta E = \|E_a - E_0\| = \|E_b - E_0\|$ is the energy splitting, and J is the coupling between the sites.

In the dimer case, I simplify each term of the interaction-frame Hamiltonian. Inspecting the $UH_\delta U^\dagger$ term:

$$U = e^{\frac{i}{\hbar}H_Dt} = \begin{pmatrix} 1 & 0 & 0 & 0 \\ 0 & e^{iw_0t} & 0 & 0 \\ 0 & 0 & e^{iw_0t} & 0 \\ 0 & 0 & 0 & e^{2iw_0t} \end{pmatrix} \tag{36}$$

$$UH_\delta U^\dagger = \begin{pmatrix} 1 & 0 & 0 & 0 \\ 0 & e^{iw_0t} & 0 & 0 \\ 0 & 0 & e^{iw_0t} & 0 \\ 0 & 0 & 0 & e^{2iw_0t} \end{pmatrix}\begin{pmatrix} 0 & 0 & 0 & 0 \\ 0 & \Delta E & J & 0 \\ 0 & J & -\Delta E & 0 \\ 0 & 0 & 0 & 0 \end{pmatrix}\begin{pmatrix} 1 & 0 & 0 & 0 \\ 0 & e^{-iw_0t} & 0 & 0 \\ 0 & 0 & e^{-iw_0t} & 0 \\ 0 & 0 & 0 & e^{-2iw_0t} \end{pmatrix} \tag{37}$$

$$= \begin{pmatrix} 0 & 0 & 0 & 0 \\ 0 & e^{iw_0t}\Delta E e^{-iw_0t} & e^{iw_0t}Je^{-iw_0t} & 0 \\ 0 & e^{iw_0t}Je^{-iw_0t} & -e^{iw_0t}\Delta E e^{-iw_0t} & 0 \\ 0 & 0 & 0 & 0 \end{pmatrix} = \begin{pmatrix} 0 & 0 & 0 & 0 \\ 0 & \Delta E & J & 0 \\ 0 & J & -\Delta E & 0 \\ 0 & 0 & 0 & 0 \end{pmatrix} = H_\delta\,. \tag{38}$$

The dipole operator $\vec{\mu}$, in any direction $\hat{n}$, will have a contribution from each site. In particular, there will be a contribution $\mu_a = \langle gg| \mu |eg\rangle = \langle ge| \mu |ee\rangle$ and $\mu_b = \langle gg| \mu |ge\rangle = \langle eg| \mu |ee\rangle$. Then, $\mu_{\hat{n}}$ takes the following form:

$$\mu_{\hat{n}} = \vec{\mu} \cdot \hat{n} = \begin{pmatrix} 0 & \mu_a^* & \mu_b^* & 0 \\ \mu_a & 0 & 0 & \mu_b^* \\ \mu_b & 0 & 0 & \mu_a^* \\ 0 & \mu_b & \mu_a & 0 \end{pmatrix} . \tag{39}$$

If the associated direction is clear, I often drop the subscript of $\mu_{\hat{n}}$. For example, the ket $|\mu\rangle$ corresponds to the dipole operator in the direction of the last pulse (see section 2.7).

I then inspect an oscillating field $\vec{E}(t) = 2V\cos(wt) = V(e^{iwt} + e^{-iwt})$. The associated $\mu_{\hat{n}}$ has normal vector $\hat{n} = \frac{\vec{E}(t)}{\|\vec{E}(t)\|}$). Consider its effects in the interaction frame:

$$U\left(\vec{\mu} \cdot \vec{E}(t)\right) U^\dagger = U\mu_{\hat{n}} 2V\cos(wt)U^\dagger = 2V\cos(wt)U\mu_{\hat{n}}U^\dagger \tag{40}$$

$$= 2V\cos(wt) \begin{pmatrix} 1 & 0 & 0 & 0 \\ 0 & e^{iw_0t} & 0 & 0 \\ 0 & 0 & e^{iw_0t} & 0 \\ 0 & 0 & 0 & e^{2iw_0t} \end{pmatrix} \begin{pmatrix} 0 & \mu_a^* & \mu_b^* & 0 \\ \mu_a & 0 & 0 & \mu_b^* \\ \mu_b & 0 & 0 & \mu_a^* \\ 0 & \mu_b & \mu_a & 0 \end{pmatrix} \begin{pmatrix} 1 & 0 & 0 & 0 \\ 0 & e^{-iw_0t} & 0 & 0 \\ 0 & 0 & e^{-iw_0t} & 0 \\ 0 & 0 & 0 & e^{-2iw_0t} \end{pmatrix} \tag{41}$$

$$= V(e^{iwt} + e^{-iwt}) \begin{pmatrix} 0 & \mu_a^* e^{-iw_0t} & \mu_b^* e^{-iw_0t} & 0 \\ \mu_a e^{iw_0t} & 0 & 0 & \mu_b^* e^{-iw_0t} \\ \mu_b e^{iw_0t} & 0 & 0 & \mu_a^* e^{-iw_0t} \\ 0 & \mu_b e^{iw_0t} & \mu_a e^{iw_0t} & 0 \end{pmatrix} \tag{42}$$

$$= V \begin{pmatrix} 0 & \mu_a^*(e^{-i(w+w_0)t} + e^{i(w-w_0)t}) & \mu_b^*(e^{-i(w+w_0)t} + e^{i(w-w_0)t}) & 0 \\ \mu_a(e^{i(w+w_0)t} + e^{-i(w-w_0)t}) & 0 & 0 & \mu_b^*(e^{-i(w+w_0)t} + e^{i(w-w_0)t}) \\ \mu_b(e^{i(w+w_0)t} + e^{-i(w-w_0)t}) & 0 & 0 & \mu_a^*(e^{-i(w+w_0)t} + e^{i(w-w_0)t}) \\ 0 & \mu_b(e^{i(w+w_0)t} + e^{-i(w-w_0)t}) & \mu_a(e^{i(w+w_0)t} + e^{-i(w-w_0)t}) & 0 \end{pmatrix} \tag{43}$$

When $w = w_0$ (the resonance condition [16]), there are terms that oscillate at frequency $2w_0$. These "counter-resonances" can be neglected in the rotating wave approximation, since they oscillate too quickly to affect the quantum state. Near resonance ($w - w_0 << w + w_0$), our Hamiltonian term simplifies to

$$U\left(\vec{\mu} \cdot \vec{E}(t)\right) U^\dagger \approx V \begin{pmatrix} 0 & \mu_a^* e^{i(w-w_0)t} & \mu_b^* e^{i(w-w_0)t} & 0 \\ \mu_a e^{-i(w-w_0)t} & 0 & 0 & \mu_b^* e^{i(w-w_0)t} \\ \mu_b e^{-i(w-w_0)t} & 0 & 0 & \mu_a^* e^{i(w-w_0)t} \\ 0 & \mu_b e^{-i(w-w_0)t} & \mu_a e^{-i(w-w_0)t} & 0 \end{pmatrix} , \tag{44}$$

which simplifies further when $w = w_0$ (the resonance condition):

$$U\left(\vec{\mu} \cdot \vec{E}(t)\right) U^\dagger \approx V \begin{pmatrix} 0 & \mu_a^* & \mu_b^* & 0 \\ \mu_a & 0 & 0 & \mu_b^* \\ \mu_b e & 0 & 0 & \mu_a^* \\ 0 & \mu_b & \mu_a & 0 \end{pmatrix} = V\mu_{\hat{n}} . \tag{45}$$

Thus, by equations 38 and 45, our interaction-frame Hamiltonian for a dimer system is simply

$$H^I(t) = UH_\delta U^\dagger + U\left(\vec{E}(t) \cdot \vec{\mu}\right) U^\dagger \approx H_\delta + V\mu_{\hat{n}} . \tag{46}$$

2.5 The Dipole Operator and Pulse Shaping

2.5.1 Decomposition of the Dipole Operator for a Dimer System

As mentioned before, μ is a Hermitian operator in Hilbert space that characterizes the strengths of transitions between various energy levels in a quantum system. Typically μ depends on the direction of the electric field. It is

sometimes denoted $\mu_{\hat{n}}$, where $\hat{n}$ corresponds to the direction of the electric field, i.e. $\vec{E} \propto \hat{n}$. The symbol $\vec{\mu}$ refers to the vector that returns $\mu_{\hat{n}}$ when dotted with some real vector $\hat{n} \in \mathbb{R}^3$. Thus,

$$\mu = \mu_{\hat{n}} = \vec{\mu} \cdot \hat{n} \tag{47}$$

I write μ as a 4×4 matrix in a dimer system, where the basis elements are $|gg\rangle, |eg\rangle, |ge\rangle, |gg\rangle$. Here, the first letter (g or e) corresponds to the energy level at the first site, and the second letter (g or e) corresponds to the energy level at the second site. Take μ to be real for this section. Then,

$$\mu = \begin{pmatrix} 0 & \mu_a & \mu_b & 0 \\ \mu_a & 0 & 0 & \mu_b \\ \mu_b & 0 & 0 & \mu_a \\ 0 & \mu_b & \mu_a & 0 \end{pmatrix} . \tag{48}$$

I assume that there is only coupling within a site, and only between adjacent energy-levels. Thus, μ_a connects adjacent energy-levels in the first site, and μ_b connects adjacent energy-levels in the second site. This is characterized by the following decomposition:

$$\sigma_x = \begin{pmatrix} 0 & 1 \\ 1 & 0 \end{pmatrix} \tag{49}$$

$$\mu = \mu_a(\mathbb{1} \otimes \sigma_x) + \mu_b(\sigma_x \otimes \mathbb{1}) \tag{50}$$

Notice how each term only projects on one subspace. In a general decomposition $A \otimes B$, A is an operator on the second site and B is an operator on the first site. This is due to the mathematical operation of the tensor (or Kronecker) product, and our choice of basis ordering in the full Hilbert space. There is an easy mnemonic to remember the operation: A is the "mask" and B is the "repeater". If A is an $m \times n$ matrix, then [4]

$$A \otimes B = \begin{pmatrix} A_{11}B & A_{12}B & \cdots & A_{1n}B \\ A_{21}B & A_{22}B & \cdots & A_{2n}B \\ \vdots & \vdots & \ddots & \vdots \\ A_{m1}B & A_{m2}B & \cdots & A_{mn}B \end{pmatrix} . \tag{51}$$

In this analogy, A "masks" the information in B. The full matrix B is "repeated" for each element of A.

Then, in the near-resonance condition ($w - w_0 << w + w_0$), equation 44 simplifies to

$$F = \begin{pmatrix} e^{i(w-w_0)t} & 0 \\ 0 & e^{-i(w-w_0)t} \end{pmatrix} \tag{52}$$

$$U\left(\vec{\mu} \cdot \vec{E}(t)\right) U^\dagger = \mu_a(\mathbb{1} \otimes F)(\mathbb{1} \otimes \sigma_x) + \mu_b(F \otimes \mathbb{1})(\sigma_x \otimes \mathbb{1}) = \mu_a(\mathbb{1} \otimes F\sigma_x) + \mu_b(F\sigma_x \otimes \mathbb{1}) . \tag{53}$$

So, the term containing μ_a only affects the subspace corresponding to the first site, and the term containing μ_b only affects the subspace corresponding to the second site.

2.5.2 Basic Pulse Shaping and the Fourier Transform

There is a broad field of designing and shaping ultrafast femtosecond pulses, and accurately producing them in laboratory settings [7] [15] [18]. Different pulse shapes will elicit different responses to the quantum system. I present a few important theorems and results.

Any function of time $f(t)$ can be represented as function of frequency $\tilde{f}(w)$ by the Fourier transform. In particular,

$$\tilde{f}(w) = \int_{-\infty}^{\infty} e^{-iwt} f(t) dt . \tag{54}$$

To reverse, I apply the inverse Fourier transform:

$$f(t) = \frac{1}{2\pi} \int_{-\infty}^{\infty} e^{iwt} f(w) dw . \tag{55}$$

Suppose $f(t) = A(t)e^{iw_0 t}$, where A is some envelope function. Then, by the Fourier shift theorem [15],

$$\tilde{f}(w) = \tilde{A}(w - w_0)\,. \tag{56}$$

Typically, there is some envelope function $A(t)$ of our electric-field pulse $E(t) = 2A(t)\cos(wt) = A(t)(e^{iwt} + e^{-iwt})$. In the simplest case, $A(t)$ is a rectangular (box-shaped) pulse:

$$A(t) = \begin{cases} V & -t_0 \leq t \leq t_0 \\ 0 & otherwise \end{cases} \tag{57}$$

The Fourier tranform of a rectangular (or boxcar) signal is defined as a *sinc* function:

$$\tilde{A}(w) = 2Vt_0 sinc(t_0 w) = \begin{cases} \frac{2Vt_0 \sin(t_0 w)}{t_0 w} & w \neq 0 \\ 2Vt_0 & w = 0 \end{cases} \tag{58}$$

So, the electric field in frequency space is

$$\tilde{E}(w) = \tilde{A}(w - w_0) + \tilde{A}(w + w_0) = 2Vt_0\left[sinc(t_0(w - w_0)) + sinc(t_0(w + w_0))\right]\,. \tag{59}$$

More commonly, Gaussian envelope shapes are used [15]. In this case, the Fourier transform preserves shape:

$$G(t) = \frac{1}{\sqrt{2\pi\sigma^2}} e^{-t^2/2\sigma^2} \tag{60}$$

$$\tilde{G}(w) = e^{-w^2\sigma^2/2}\,. \tag{61}$$

Thus, if the electric field has a Gaussian envelope (i.e. $E(t) = 2G(t)\cos(wt)$), then

$$\tilde{E}(w) = \tilde{G}(w - w_0) + \tilde{G}(w + w_0) = e^{-(w-w_0)^2\sigma^2/2} + e^{-(w+w_0)^2\sigma^2/2}\,. \tag{62}$$

In the "sudden pulse" or "semi-impulsive" approximation, the envelope is modeled as a Dirac delta "function" [12]. The Dirac delta $\delta(t)$ has two properties: (1) that $\delta(t) = 0$ if $t \neq 0$ and (2) the integral $\int_{-\infty}^{\infty} \delta(t) = 1$. If the envelope is proportional to the Dirac delta:

$$D(t) = D\delta(t) \tag{63}$$

$$\tilde{D}(w) = D \tag{64}$$

The Fourier transform of the Dirac delta is constant at all frequencies. Thus, if the electric field had a Dirac delta envelope (i.e. $E(t) = 2D(t)\cos(wt)$), then

$$\tilde{E}(w) = \tilde{D}(w - w_0) + \tilde{D}(w + w_0) = 2D\,. \tag{65}$$

With this approximation, the electric field has constant amplitude at all frequencies.

2.6 Linear and Bilinear Control Theory

In control theory, standard state-space representation of a bilinear system has the following form [10]:

$$\dot{\mathbf{x}}(t) = A(t)\mathbf{x}(t) + B(t)\vec{u}(t) + \sum_{i=1}^{r} N_i(t)\mathbf{x}(t)u_i(t) \tag{66}$$

$$y(t) = C(t)\mathbf{x}(t) + D(t)\vec{u}(t) \tag{67}$$

Here, $\mathbf{x}(t)$ is the "state" or "state vector", $\vec{u}(t)$ is the "input" (with r entries), and $y(t)$ is the "output". The matrices A, B, N_i evolve the initial state into a future state, while C, D are used for the "measurement". In particular, linear system has $N_i = 0$ for all i, and a time-invariant system has no time-dependence in the matrices. These special types of bilinear systems are much simpler to solve than the general case [10].

Consider our state vector as $\mathbf{x}(t) \in \mathbb{S}_{4n^2}$. The natural choice for output $y(t)$ is a measurable function of time — the scalar polarization measurement $P_3(t) \in \mathbb{C}$. Then, $C(t) = \mathbf{C}^\dagger = (0 \quad 0 \quad 0 \quad \langle\mu|)$, and $D(t) = \mathbf{0}$. It would be

simple to use a time-dependent $A(t)$ matrix for the evolution of $\mathbf{x}(t)$ (equation 66), but the problem is significantly easier if the system is time-invariant. (This requires all matrices A, B, C, D, N_i to be time-independent.)

In general, the Hamiltonian's time dependence comes from electric-field interactions: $H(t) = H_0 + \vec{E}(t) \cdot \vec{\mu} = H_D + H_\delta + \vec{E}(t) \cdot \vec{\mu}$. This electric field $\vec{E}(t)$ is most easily identified as the input $\vec{u}(t)$. Let us define superoperators (i.e. in Liouville space) $M_D, M_\delta, M_{\hat{n}} \in \mathcal{L}(\mathbb{L}_{n^2})$ in the following way:

$$\hat{\hat{M}}_D \cdot = \frac{-i}{\hbar} \hat{\hat{H}}_D \cdot \iff \frac{-i}{\hbar} [\hat{H}_D, \cdot] \tag{68}$$

$$\hat{\hat{M}}_\delta \cdot = \frac{-i}{\hbar} \hat{\hat{H}}_\delta \cdot \iff \frac{-i}{\hbar} [\hat{H}_\delta, \cdot] \tag{69}$$

$$(\forall \hat{n} \in \mathbb{R}^3)\, , \hat{\hat{M}}_{\hat{n}} \cdot = \frac{-i}{\hbar} \hat{\hat{\mu}}_{\hat{n}} \cdot \iff \frac{-i}{\hbar} [\hat{H}_{\hat{n}}, \cdot] \tag{70}$$

Recall that one can represent the commutator operation in Hilbert space with a superoperator in Liouville space.

From here, I construct superoperators $M(t), M_0 \in \mathcal{L}(\mathbb{L}_{n^2})$:

$$M(t) = M_D + M_\delta + \sum_{i \in [\vec{x}, \vec{y}, \vec{z}]} E_i(t) M_i(t) \tag{71}$$

$$M_0 = M_D + M_\delta \tag{72}$$

By linearity of the commutator, $M(t)\cdot$ and $M_0 \cdot$ represent $\frac{-i}{\hbar}[H(t), \cdot]$ and $\frac{-i}{\hbar}[H_0, \cdot]$ in Hilbert space, respectively.

There remains coupling between $\mathbf{x}(t)$ and $E(t)$. In particular, $\mathbf{x}$ evolves as

$$\dot{\mathbf{x}}(t) = A_D \mathbf{x}(t) + A_\delta \mathbf{x}(t) + \sum_i N_i \mathbf{x}(t) u_i(t) \tag{73}$$

$$= \begin{pmatrix} 0 & 0 & 0 & 0 \\ M_D & 0 & 0 & 0 \\ 0 & M_D & 0 & 0 \\ 0 & 0 & M_D & 0 \end{pmatrix} \mathbf{x}(t) + \begin{pmatrix} 0 & 0 & 0 & 0 \\ M_\delta & 0 & 0 & 0 \\ 0 & M_\delta & 0 & 0 \\ 0 & 0 & M_\delta & 0 \end{pmatrix} \mathbf{x}(t) + \sum_{i \in [\vec{x}, \vec{y}, \vec{z}]} \begin{pmatrix} 0 & 0 & 0 & 0 \\ M_i & 0 & 0 & 0 \\ 0 & M_i & 0 & 0 \\ 0 & 0 & M_i & 0 \end{pmatrix} \mathbf{x}(t) E_i(t)\, . \tag{74}$$

I define extended superoperators $A_D, A_\delta, N_{\hat{n}} \in \mathcal{L}(\mathbb{S}_{4n^2})$ implicitly in the equation above. (Recall that extraneous symbols were dropped from vectors and matrices.) The vector $\vec{E}(t)$ has three entries ($[\vec{x}, \vec{y}, \vec{z}]$), paired with $[N_{\vec{x}}, N_{\vec{y}}, N_{\vec{z}}]$, respectively. I compare the above with equations 13, 66, and 67 to define the rest of the terms in a bilinear control problem. Summarizing:

$$y(t) = P_3(t) \tag{75}$$

$$\vec{u}(t) = \vec{E}(t) \tag{76}$$

$$A = A_D + A_\delta \tag{77}$$

$$B = D = 0 \tag{78}$$

$$C = \mathbf{C}^\dagger\, . \tag{79}$$

The problem is now in the form of a bilinear, time-invariant system.

2.7 Solving the Free Evolution System for Third-Order Polarization (in Lab Frame)

In general, third-order spectroscopy experiments employ four-wave mixing: at time $t = t_0$, an electric pulse excites a molecule in its ground state. Two more pulses fire at the molecule (at time t_1 and t_2), adjusting the molecular state. A last pulse (at time t_3) is designed such that the molecule is forced back into its ground state, emitting some measurable electric field. This last pulse is the "measurement".

In a classical controls context, the input $\vec{u}(t)$ models the electric field $\vec{E}(t)$. So, $\vec{u}(t)$ is pulse-like at $t = t_0, t_1, t_2$, and 0 everywhere else. (Since the last pulse manifests as the measurement operator C, there are effectively no inputs after time $t = t_2$).

Without electric-field impulses, the system evolves linearly:

$$\dot{\mathbf{x}}(t) = A\mathbf{x}(t) = \begin{pmatrix} 0 & 0 & 0 & 0 \\ M_0 & 0 & 0 & 0 \\ 0 & M_0 & 0 & 0 \\ 0 & 0 & M_0 & 0 \end{pmatrix} \mathbf{x}(t) \tag{80}$$

$$y(t) = C\mathbf{x}(t) = (0 \quad 0 \quad 0 \quad \langle\mu|)\mathbf{x}(t) \tag{81}$$

(Recall that $M_0 = M_D + M_\delta$.) Let's investigate the closed-form solution to this linear system, which is

$$\mathbf{x}(t + t_0) = e^{At}\mathbf{x}(t_0)\,. \tag{82}$$

Here, e^A is shorthand for its series expansion

$$e^A = (I + A + A^2/2 + A^3/6 + ...)\,. \tag{83}$$

Since the extended superoperator A is nilpotent, e^A has a finite number of terms. In particular, $A^4 = 0$, so

$$e^{At} = \begin{pmatrix} 1 & 0 & 0 & 0 \\ M_0 t & 1 & 0 & 0 \\ \frac{1}{2}M_0^2 t^2 & M_0 t & 1 & 0 \\ \frac{1}{6}M_0^3 t^3 & \frac{1}{2}M_0^2 t^2 & M_0 t & 1 \end{pmatrix}\,. \tag{84}$$

Since $y(t) = (0 \quad 0 \quad 0 \quad \langle\mu|)\mathbf{x}(t)$, the closed-form solution for $y(t + t_0) = P_3(t + t_0)$ is

$$P_3(t + t_0) = y(t + t_0) = \langle\mu|\,(M_0^3 t^3/6 \quad M_0^2 t^2/2 \quad M_0 t \quad 1)\mathbf{x}(t_0)\,. \tag{85}$$

Expanding $\mathbf{x}(t_0)$ in terms of its perturbation components, the above equation simplifies to

$$P_3(t + t_0) = y(t + t_0) = \langle\mu|\left(M_0^3 t^3/6\,|\rho_0(t_0)\rangle + M_0^2 t^2/2\,|\rho_1(t_0)\rangle + M_0 t\,|\rho_2(t_0)\rangle + |\rho_3(t_0)\rangle\right)\,. \tag{86}$$

At small t (where the perturbative expansion is valid), the output polarization is a cubic function of time. This is an effective model of quantum state evolution between the pulses (when $\vec{E}(t) = \vec{0}$).

2.8 Solving the General (Bilinear) System for Third-Order Polarization

2.8.1 Box-shaped Pulses

I solve the system more generally with an important approximation [10, 11]: $\vec{E}(t)$ is a series of box-shaped pulses, at fixed amplitude $2V$, for a short duration $\Delta t << t_1, t_2, t_3$. With this approximation (and the rotating wave approximation), the system is approximately linear. In particular, the evolution equation in the interaction frame (equation 33) is

$$\frac{\partial \rho_n^I(t)}{\partial t} = -\frac{i}{\hbar}[H_\delta + V\mu_{\hat{n}}, \rho_{n-1}^I(t)]\,. \tag{87}$$

In a similar manner to equation 74, the state evolution behaves as

$$\dot{\mathbf{x}}^I(t) = (A_\delta + VN_{\hat{n}})\mathbf{x}^I(t) = \begin{pmatrix} 0 & 0 & 0 & 0 \\ M_\delta + VM_{\hat{n}} & 0 & 0 & 0 \\ 0 & M_\delta + VM_{\hat{n}} & 0 & 0 \\ 0 & 0 & M_\delta + VM_{\hat{n}} & 0 \end{pmatrix} \mathbf{x}(t)\,. \tag{88}$$

Between pulses, there is no electric-field component, and the interaction-frame evolution equation simplifies to

$$\dot{\mathbf{x}}^I(t) = A_\delta \mathbf{x}^I(t)\,. \tag{89}$$

So, the state evolves between pulses as

$$\mathbf{x}^I(t+t_0) = e^{A_\delta t}\mathbf{x}^I(t_0) \tag{90}$$

$$e^{A_\delta t} = \begin{pmatrix} 1 & 0 & 0 & 0 \\ M_\delta t & 1 & 0 & 0 \\ \frac{1}{2}M_\delta^2 t^2 & M_\delta t & 1 & 0 \\ \frac{1}{6}M_\delta^3 t^3 & \frac{1}{2}M_\delta^2 t^2 & M_\delta t & 1 \end{pmatrix} . \tag{91}$$

During the pulse is a bit more complicated. I assume $\hat{n}$ is in the direction of the electric field pulse $\vec{E}$.

By the box-shaped pulse approximation, V is time-independent for the duration (Δt) of the pulse. I apply the same analysis as before:

$$\mathbf{x}^I(t_0+\Delta t) = e^{(A_\delta + VN_{\hat{n}})\Delta t}\mathbf{x}^I(t_0) \tag{92}$$

$$e^{(A_\delta + VN_{\hat{n}})\Delta t} = \begin{pmatrix} 1 & 0 & 0 & 0 \\ (M_\delta + VM_{\hat{n}})\Delta t & 1 & 0 & 0 \\ \frac{1}{2}(M_\delta + VM_{\hat{n}})^2\Delta t^2 & (M_\delta + VM_{\hat{n}})\Delta t & 1 & 0 \\ \frac{1}{6}(M_\delta + VM_{\hat{n}})^3\Delta t^3 & \frac{1}{2}(M_\delta + VM_{\hat{n}})^2\Delta t^2 & (M_\delta + VM_{\hat{n}})\Delta t & 1 \end{pmatrix} . \tag{93}$$

I now have a linear equation describing the final state $\mathbf{x}^I(t)$ from the initial state:

$$\mathbf{x}^I(t_3) = e^{A_\delta(t_3-t_2)}e^{(A_\delta + VN_{\hat{n}})\Delta t}\mathbf{x}^I(t_2) \tag{94}$$

$$= e^{A_\delta(t_3-t_2)}e^{(A_\delta + VN_{\hat{n}})\Delta t}e^{A_\delta(t_2-t_1)}e^{(A_\delta + VN_{\hat{n}})\Delta t}\mathbf{x}^I(t_1) \tag{95}$$

$$= e^{A_\delta(t_3-t_2)}e^{(A_\delta + VN_{\hat{n}})\Delta t}e^{A_\delta(t_2-t_1)}e^{(A_\delta + VN_{\hat{n}})\Delta t}e^{A_\delta(t_1-t_0)}e^{(A_\delta + VN_{\hat{n}})\Delta t}\mathbf{x}^I(t_0) . \tag{96}$$

Converting to and from the interaction frame is easy, as shown by equations 23 and 25. I do that here, as

$$\mathbf{x}(t_3) = Q_D^\dagger(t_3)e^{A_\delta(t_3-t_2)}e^{(A_\delta + VN_{\hat{n}})\Delta t}e^{A_\delta(t_2-t_1)}e^{(A_\delta + VN_{\hat{n}})\Delta t}e^{A_\delta(t_1-t_0)}e^{(A_\delta + VN_{\hat{n}})\Delta t}Q_D(t_0)\mathbf{x}(t_0) . \tag{97}$$

The polarization output $y(t) = P_3(t)$ is described by

$$y(t_3) = C\mathbf{x}(t_3) = \begin{pmatrix} 0 & 0 & 0 & \langle\mu| \end{pmatrix} \begin{pmatrix} |\rho_0(t_3)\rangle \\ |\rho_1(t_3)\rangle \\ |\rho_2(t_3)\rangle \\ |\rho_3(t_3)\rangle \end{pmatrix} = \langle\mu|\rho_3(t_3)\rangle = tr(\mu\rho_3(t_3)) . \tag{98}$$

2.8.2 Dirac Delta Pulses

In he semi-impulsive limit (by modeling each pulses with a Dirac delta), the equation is slightly simpler. This can be done in two ways: Re-integrate the recursive equation of motion (equation 33) or shrink the box-pulse so in the limit it approaches a Dirac delta pulse.

The first method approximates the impulse $V(t)$ as a Dirac delta $D\delta(t-t_0)$. When integrated,

$$\rho_n^I(t_{0+}) - \rho_n^I(t_{0-}) = \int_{t_{0-}}^{t_{0+}} dt \frac{\partial\rho_n^I(t)}{\partial t} = \int_{t_{0-}}^{t_{0+}} dt - \frac{i}{\hbar}[H_\delta + V(t)\mu_{\hat{n}}, \rho_{n-1}^I(t)] \approx \frac{-i}{\hbar}[D\mu_{\hat{n}}, \rho_{n-1}^I(t_0)] . \tag{99}$$

At time t_0, the value of the Dirac delta is much greater than H_δ, so the term drops out. This method is akin to applying the dipole operator directly onto the state. Bringing this up to extended Liouville space,

$$\mathbf{x}^I(t_{0+}) = \mathbf{x}^I(t_{0-}) + DN_{\hat{n}}\mathbf{x}^I(t_{0-}) = (1 + DN_{\hat{n}})\mathbf{x}^I(t_{0-}) . \tag{100}$$

In this limit, the Dirac delta pulse corresponds to the extended Liouville operator $(1 + DN_{\hat{n}})$.

The second method keeps $D = V\Delta t$ constant but takes $V \to \infty$ and $\Delta t \to 0$. This turns equation 92 into

$$\lim_{V\to\infty,\Delta t\to 0} \mathbf{x}^I(t_0+\Delta t) = \lim_{V\to\infty,\Delta t\to 0} e^{(A_\delta + VN_{\hat{n}})\Delta t}\mathbf{x}^I(t_0) = e^{VN_{\hat{n}}\Delta t}\mathbf{x}^I(t_0) . \tag{101}$$

During the pulse, the equation is no longer dependent on A_δ. The expansion for the exponential also simplifies to

$$e^{VN_{\hat{n}}\Delta t} = \begin{pmatrix} 1 & 0 & 0 & 0 \\ VM_{\hat{n}}\Delta t & 1 & 0 & 0 \\ \frac{1}{2}(VM_{\hat{n}})^2\Delta t^2 & VM_{\hat{n}}\Delta t & 1 & 0 \\ \frac{1}{6}(VM_{\hat{n}})^3\Delta t^3 & \frac{1}{2}(VM_{\hat{n}})^2\Delta t^2 & VM_{\hat{n}}\Delta t & 1 \end{pmatrix} . \tag{102}$$

It is easy to rewrite the full equations of motion (equations 97 and 98). Substitute each occurrence of the box-shaped pulse term $e^{(A_\delta + VN_{\hat{n}})\Delta t}$ out with our Dirac delta pulse term ($(1 + DN_{\hat{n}})$ or $e^{VN_{\hat{n}}\Delta t}$) from this section.

3 Algorithms

I implemented algorithms using the Python programming language and Jupyter notebook [13] to implement and solve the linear equations 97 and 98. The source code is available upon request.

I first simulated the "forward motion" of the quantum state, evolving an initial ground state through the pulses and conducting the measurement (as in equation 98). I chose relevant physical parameters for a dimer system [18] and varied the times between pulses. I then plotted my polarization data in time-space (as a function of t_1, t_3) and in frequency-space (as a function of w_1, w_3). In particular, this required exponentiation of matrices with a special form (as in equation 84). Additionally, U and Q_D were easy to construct, since they are diagonal.

I also wrote inversion software to find physical parameters (some of $\mu, J, \Delta E$) from the output polarization state $P_3(t) = Y(t)$, given pulse separation times t_1, t_2, t_3, and all other physical parameters. Because the problem is non-convex, I used gradient descent methods to find these values. Gradient descent is an iterative method that tries to find the values for variables $\vec{x}$ that minimize some cost function $C(\vec{x})$. In particular, it computes the gradient of the cost function and updates the guesses repeatedly until satisfying a convergence condition. Typically, the update scheme is defined as

$$\vec{x}^{(n+1)} = \vec{x}^{(n)} - \epsilon \frac{\partial C}{\partial \vec{x}}\Big|_{\vec{x}=\vec{x}^{(n)}} , \tag{103}$$

where ϵ is the "learning rate" of the algorithm [2]. A larger ϵ will elicit larger changes in the guesses for $\vec{x}$. This value can be tuned for a particular problem.

In the space of learning and optimization methods, gradient descent is a simple algorithm. More sophisticated methods may have better success, like the Alternating Direction Method of Multipliers (ADMM) [3].

4 Code Use

All code from this project is available upon request.

The first portion tests this theory against the open-source Python package *Qspectra* [6]. This simulation package is meant for for nonlinear spectroscopy signals on molecular aggregates, and is designed to solve approximate models of open quantum systems. The code I use from this package is the third-order-response function, which produces response output data based on physical parameters. (*Qspectra* assumes delta-function pulses, so the response plot and the polarization plots are proportional.)

In my code, I implement the above evolution equations (equations 97 and 98). One inputs the same physical parameters ($\vec{E}, H_0, \mu, t_1, t_2, t_3$) and the output is the polarization $y(t)$, discretized over each time variable t_1, t_2, t_3. This has the same form as *Qspectra*, so I comare the 2D plots in frequency-space and the associated diagonal absorption spectrum.

The second portion contains an iterative solver to solve for components of μ (in particular, the values of μ_a and μ_b). The input here is all other physical parameters of the system ($\vec{E}, H_0, t_1, t_2, t_3$) and the polarization data $y(t)$. This is close to the classic inversion problem $Ax = b$, except the goal is to solve for parts of A instead of x. I use gradient descent to find the best choice of μ that minimizes the difference between $P_3(\mu)$ and the correct polarization data $P_3(\mu^*)$. This is an iterative process that converges when the difference is below a specified threshold.

Figure 1: *Qspectra*-simulated 2D frequency plot for a dimer system.

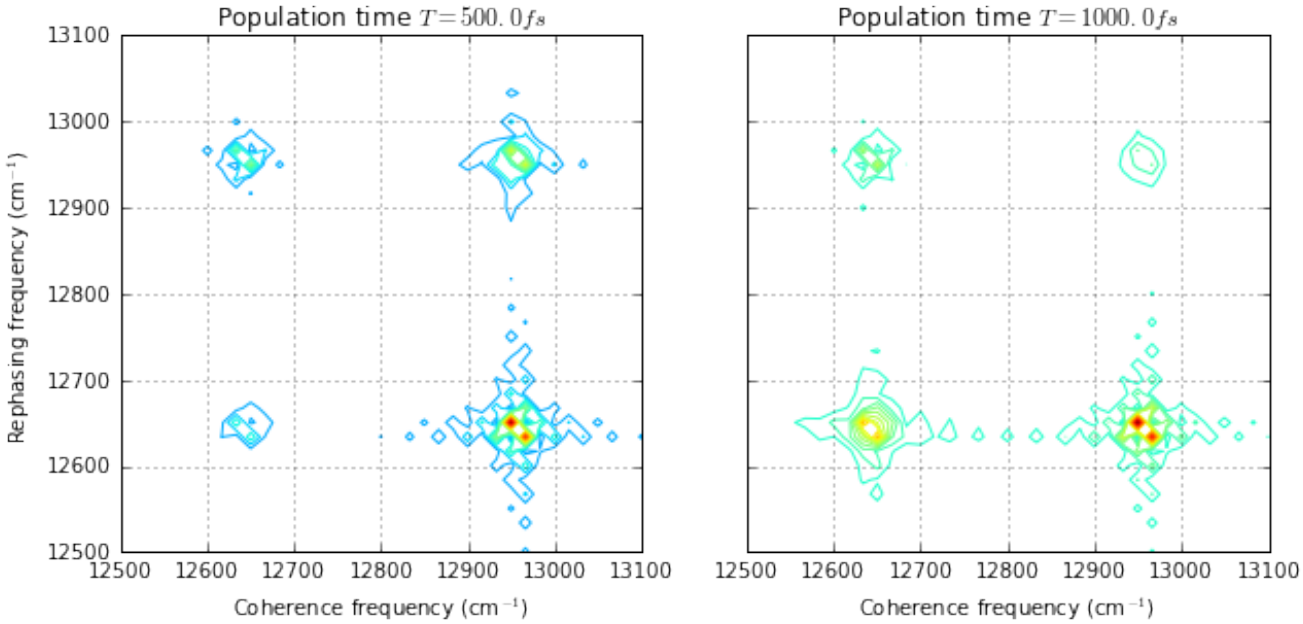

5 Test Problems and Results

5.1 A Test Application: The Dimer system

I test the success of my process on a simple dimer system (i.e. $n = 2$ energy levels). I use the system parameters from Yuen-Zhou et. al. [18] as input for my code:

$$\mu_a = (1 \quad 0 \quad 0)^\top \tag{104}$$

$$\mu_b = (2\cos(0.3) \quad 2\sin(0.3) \quad 0)^\top \tag{105}$$

$$E_a = 12719 \tag{106}$$

$$E_b = 12881 \tag{107}$$

$$J = 120 \tag{108}$$

$$0 \leq t_1, t_2, t_3 \leq 1000\,. \tag{109}$$

Here, the dipole moments (μ_a and μ_b) are in units of Debye, the time variables (t_1, t_2, t_3) are in units of femtoseconds, and the energies and couplings (E_a, E_b, J) are in units of wavenumbers.

I first generate polarization output to compare with the data generated from *Qspectra*. I created 2D frequency plots, as done in the standard literature [12], which should match plots generated by *Qspectra*. *Qspectra*'s plots are shown in Figure 1. Notice that there are usually four peaks: two along the diagonal and two on the off-diagonal. Each x-value and y-value is the oscillating frequency of one of the excited states.

My plots in frequency space are shown in Figure 2. I assume short (55 femtosecond) box-shaped pulses. There is an unusually large spike at the center frequency. Notice that there are peaks that mimic *Qspectra*'s peaks but also other spurious peaks in the plots. These could correspond to absorption at frequencies near the excited-state energies. It is possible that this phenomenon is from numerical errors in the Fourier transform.

Overall, the plots behave some similarities, which is promising for the approach.

A perhaps more useful plot is the diagonal absorption spectrum, which should peak at the energies of the excited states. The eigenvalues of this system correspond to frequencies of 12644 and 12956 cm^{-1}. *Qspectra*'s spectrum in Figure 3 shows sharp peaks at these frequencies, likely due to the delta-pulse approximations in simulation. We do expect some broadening to occur.

Figure 2: My own simulated 2D frequency plot for a dimer system.

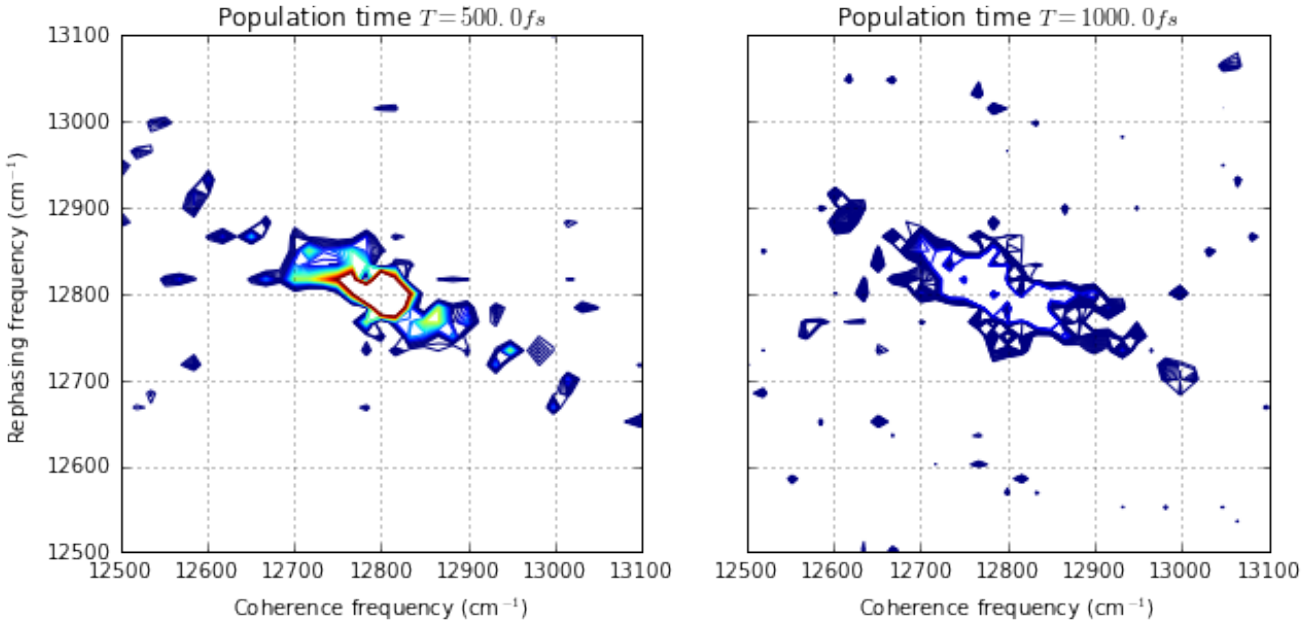

Figure 3: *Qspectra*-simulated absorption spectrum for a dimer system.

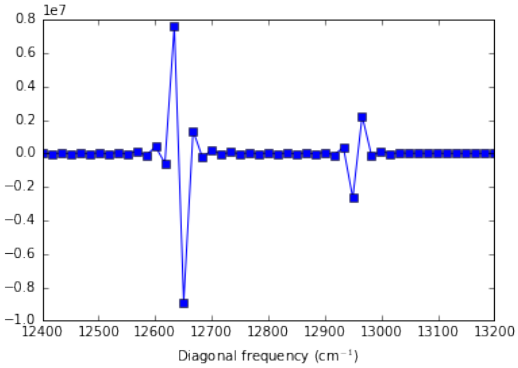

Figure 4: My own simulated absorption spectrum for a dimer system.

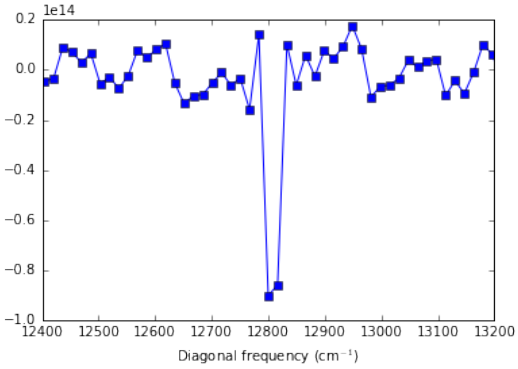

In contrast, my plots in Figure 4 show the large peak at the average frequency , as well as other peaks throughout the plot. There are small spikes at the expected frequencies ($12644, 12956$ cm^{-1}), but it is unlikely that light at 12500 cm^{-1} was absorbed by the system. There must be some extra spiking due to one of my approximations — likely, the box-pulse approximation. With pulses modeled as Dirac delta, I should get better agreement between the figures.

The second portion to iteratively solve for parameters is so far unsuccessful. I initially attempted to find μ_a and μ_b from output data. In Figure 5(a), I vary μ_a and μ_b, showing that $P_3(\mu_a, \mu_b)$ is clearly non-convex. So, there is no guarantee of convergence, which makes it more difficult to solve.

Next, I tried gradient descent, approximating the gradient with the built-in algorithm from Python package *scipy* [9]. Unfortunately, there were convergence issues — I kept getting stuck in local minima. This was because the cost rapidly oscillated with adjustments in μ. As shown in Figure 5(b), it is unlikely that gradient descent will converge to the correct answer.

The parameter estimation hinges on a successful inversion of the linear system. Other non-convex iterative learning method may work here [14]. If the guess is initialized close to the actual value, the solution is more likely to find the correct answer.

5.2 Possibilities for Future Work

Overall, this is a novel approach to studying nonlinear spectroscopy problems, and analyzing the evolution of perturbative expansions. In particular, equations 7, 11, 33, and 84, and 97 are novel and

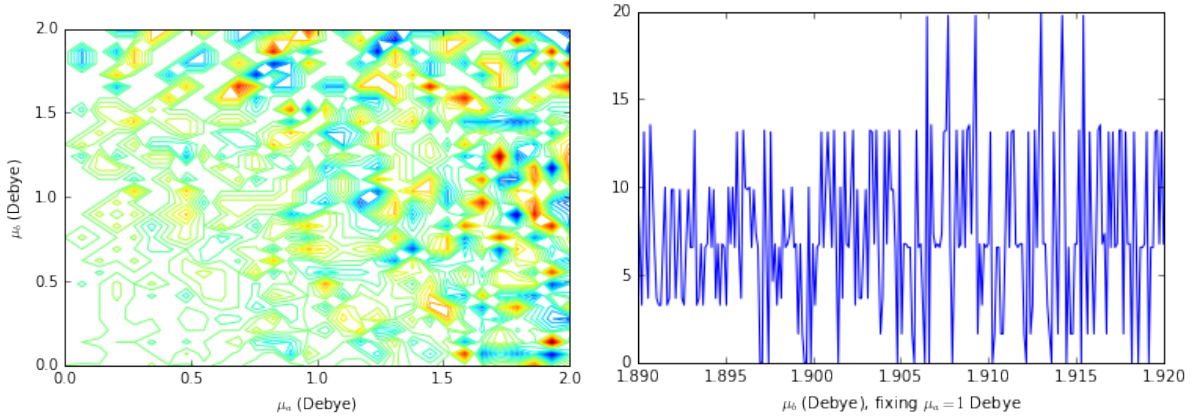

(a) Contour plot of P_3 varying μ_a, μ_b.

(b) Error $\|P_3(\mu_b) - P_3(\mu_b^*)\|$ versus μ_b. ($\mu_b^* \approx 1.9106$ Debye)

Figure 5: My inversion attempt to retrieve μ from $P_3(t)$ ($t_1 = t_2 = t_3 = 100fs$).

worth exploring. Control theory is a rich body of knowledge to support future theoretical and computational attempts at solving similar problems.

Future theoretical work can relax assumptions made during this derivation, particularly the single-frequency electric field pulse (resonance condition) in equation 45. While a box-shaped filter removes time-dependence from the term, a Gaussian filter is more often used in experiment [15] [18]. This control-theoretic approach can also solve for higher-order polarization terms by expanding the extended Liouville space. The recursive formulation of the von-Neumann equation (equation 7) could have implications in any experiment where a quantum system experiences a perturbation.

Fundamentally, I have created a vector space where explicit linear equations transform the initial quantum state to its final state and from final state to output polarization. This is done by going beyond the Liouville space into an extended Liouville space and by writing the von-Neumann equation in a recursive form. This space and set of equations can be used for other systems besides the dimer, like the 7-level FMO system [8]. More investigation into the discrepancies between plots generated by these equations and *Qspectra*'s plot is warranted.

Parameter estimation of μ, J, and/or ΔE hinges solely on inversion of a linear equation, comparable to the pump-probe inversion done in [7]. More sophisticated iterative inversion processes may produce better results and/or quicker convergence of these terms [14]. This method may be the most direct way to extract physical Hamiltonian parameters — a novel approach at the classic "inversion problem".

6 Acknowledgements

I thank Robert Kosut from SC Solutions for several insights during brainstorming sessions on reducing a nonlinear problem to a bilinear problem, as well as for suggesting optimization softwares and solution methods for a variety of differential equations throughout the process. I also thank Donghyun Lee and Siva Darbha for preliminary conversations about nonlinear spectroscopy and for discussions about *Qspectra* and my own code. Thanks to Jeffrey Epstein and Daniel Freeman for guidance and general advice on conducting theoretical research.

References

[1] M. S. Anwar. Superoperators in NMR. URL `https://physlab.lums.edu.pk/images/4/46/Superop.pdf`.

[2] S. Boyd and L. Vandenberghe. *Convex Optimization*. Cambridge University Press, Cambridge, UK ; New York, 1 edition edition, Mar. 2004. ISBN 978-0-521-83378-3.

[3] S. Boyd, N. Parikh, E. Chu, B. Peleato, and J. Eckstein. Distributed Optimization and Statistical Learning via the Alternating Direction Method of Multipliers. *Found. Trends Mach. Learn.*, 3(1):1–122, Jan. 2011. ISSN 1935-8237. doi: 10.1561/2200000016. URL http://dx.doi.org/10.1561/2200000016.

[4] H.-P. Breuer and F. Petruccione. *The Theory of Open Quantum Systems*. Oxford University Press, 2002. ISBN 9780198520634.

[5] S. J. Devitt, J. H. Cole, and L. C. L. Hollenberg. Scheme for direct measurement of a general two-qubit Hamiltonian. *Physical Review A*, 73(5):052317, May 2006. doi: 10.1103/PhysRevA.73.052317. URL http://link.aps.org/doi/10.1103/PhysRevA.73.052317.

[6] S. Hoyer. shoyer/qspectra. URL https://github.com/shoyer/qspectra.

[7] S. Hoyer and K. B. Whaley. Inverting pump-probe spectroscopy for state tomography of excitonic systems. *The Journal of Chemical Physics*, 138(16):164102, Apr. 2013. ISSN 0021-9606, 1089-7690. doi: 10.1063/1.4800800. URL http://scitation.aip.org/content/aip/journal/jcp/138/16/10.1063/1.4800800.

[8] S. Hoyer, F. Caruso, S. Montangero, M. Sarovar, T. Calarco, M. B. Plenio, and K. B. Whaley. Realistic and verifiable coherent control of excitonic states in a light harvesting complex. *New Journal of Physics*, 16(4): 045007, Apr. 2014. ISSN 1367-2630. doi: 10.1088/1367-2630/16/4/045007. URL http://arxiv.org/abs/1307.4807. arXiv: 1307.4807.

[9] E. Jones, T. Oliphant, P. Peterson, et al. SciPy: Open source scientific tools for Python, 2001–. URL http://www.scipy.org/. [Online; accessed 2016-05-10].

[10] J.-N. Juang. Continuous-Time Bilinear System Identification. *Nonlinear Dynamics*, 39(1-2):79–94, Jan. 2005. ISSN 0924-090X, 1573-269X. doi: 10.1007/s11071-005-1915-z. URL http://link.springer.com/article/10.1007/s11071-005-1915-z.

[11] M. Majji. *System Identification: Time Varying and Nonlinear Methods*. July 2010. URL http://oaktrust.library.tamu.edu/handle/1969.1/ETD-TAMU-2009-05-637.

[12] S. Mukamel. *Principles of Nonlinear Optical Spectroscopy*. Oxford University Press, 1999. ISBN 9780195132915.

[13] F. Pérez and B. E. Granger. IPython: a system for interactive scientific computing. *Computing in Science and Engineering*, 9(3):21–29, May 2007. ISSN 1521-9615. doi: 10.1109/MCSE.2007.53. URL http://ipython.org.

[14] Y. Saad. *Iterative Methods for Sparse Linear Systems, Second Edition*. Society for Industrial and Applied Mathematics, Philadelphia, 2 edition edition, Apr. 2003. ISBN 978-0-89871-534-7.

[15] R. Trebino. *Frequency-Resolved Optical Gating: The Measurement of Ultrashort Laser Pulses*. Springer US, Boston, MA, 2000. ISBN 978-1-4613-5432-1 978-1-4615-1181-6. URL http://link.springer.com/10.1007/978-1-4615-1181-6.

[16] K. Young. Spin Resonance. URL http://inst.eecs.berkeley.edu/~cs191/fa14/lectures/lecture4.pdf.

[17] K. C. Young, M. Sarovar, R. Kosut, and K. B. Whaley. Optimal quantum multiparameter estimation and application to dipole- and exchange-coupled qubits. *Physical Review A*, 79(6):062301, June 2009. doi: 10.1103/PhysRevA.79.062301. URL http://link.aps.org/doi/10.1103/PhysRevA.79.062301.

[18] J. Yuen-Zhou, J. J. Krich, M. Mohseni, and A. Aspuru-Guzik. Quantum State and Process Tomography of Energy Transfer Systems via Ultrafast Spectroscopy. *Proceedings of the National Academy of Sciences*, 108(43):17615–17620, Oct. 2011. ISSN 0027-8424, 1091-6490. doi: 10.1073/pnas.1110642108. URL http://arxiv.org/abs/1006.4866. arXiv: 1006.4866.